Scientia Africana, Vol. 14 (No.1), June 2015. Pp 165-177
 ISSN 1118 – 1931

ON THE THIRD-ORDER COEFFICIENTS OF THE TAIL OF THE DIRECT CORRELATION FUNCTION: NEW COMPUTATIONAL DIRECTION

K. O. Monago

Department of Pure and Industrial Chemistry
University of Port Harcourt
P M B 5323 Choba, Port Harcourt

Received: 06-01-15
Accepted:15-06-15

ABSTRACT

A practical scheme is here presented for the numerical calculation of the tail of the direct correlation function. The procedure is shown to lead to accurate values for all the rooted cluster integrals in the tail function which are proportional to ρ^3. The derived expressions are shown to be correct and reliable at all temperatures by comparison with the known analytical results for the Gaussian potential function and certain irreducible cluster diagrams that occur in the 5th virial coefficient.

INTRODUCTION

Integral-equation methods are analytical theories of fluid structure which offer prescriptions for the quantitative determination of spatial correlation functions. These methods have well-founded theoretical bases but unlike the virial equation of state lead to useful, if not accurate, results at liquid densities and unlike computer simulation methods require modest computation to implement.

Of the integral-equations that are based on the Ornstein-Zernike (OZ) equation, there are two modern paths by which these methods can be extended to higher density states. The first, the "unique functionality" approximation is empirical and is motivated by the observation that many integral-equation theories in the OZ class approximate their bridge function, $E(r)$, or equivalently the tail function, $d(r)$, by a simple function of the cavity function, $y(r)$ (Duh and Henderson, 1996; Varlet, 1980). Results from computer simulation show that the unique functionality approximation is better fulfilled in predominantly repulsive potentials and less so in potentials with attractive sections. However, it turns out that for realistic potentials, a new function, $s(r)$, defined by:

$$s(r) = h(r) - c(r) - \phi_a / kT \qquad (1)$$

may be postulated which approximately obeys the unique functionality assumption (Duh and Haymet, 1995). In equation (1), $h(r)$ and $c(r)$ are, respectively, the total and direct correlation functions; ϕ_a is a function which is related to the attractive section of a realistic potential, T is the thermodynamic temperature and k is the Boltzmann constant. For the present purpose, it should be noted that the unique functionality approximation is not exact at low gas densities.

An alternative path to higher order approximations uses inhomogeneous fluid

theory. This approach assumes the presence of a fluid particle at the origin, identical with the rest of the other particles in a one-component fluid, which is the source of inhomogeneity (Henderson, 1992; Attard, 1989; Duh and Henderson, 1997). The usual equations in the integral-equation methodology for a homogeneous fluid are now applied to this system, except that one uses the local density instead of that in the bulk. An extra equation is now also required which relates the inhomogeneous pair correlation function to the homogeneous analogue. The resulting approximation is exact up to the additive fourth virial coefficient and, in that respect, is equivalent to the older, cumbersome PY2 and HNC2 methods of Varlet (1980) and Wertheim (1967), but without the disadvantages of either. However, all three methods suffer from the disadvantage that considerable computational resources are required to implement them.

The functions $d(r)$ and $E(r)$ may be represented as power series in density the coefficients of which, in the case of an additive interaction, are well-known. Hence, an alternative path to extended theories is to replace the unknown function $d(r)$ (or, alternatively, $E(r)$) with their first few calculable coefficients in its power series expansion in density.

There have been other attempts to calculate the graphs in $E(r)$ which are proportional to ρ^3. Kim et al. (1967; 1969) first derived integrated expressions for the graphs, but their implementation particularly of the complete, rooted five-molecule graph for a Lennard-Jones potentials led to inaccurate results at low temperature. More recently, Attard and Patey (1990) derived integrated expressions for the graphs in $E(r)$ correct to the third-order in density but provided no numerical values for any of the graphs.

Theory

We are interested in a theory of non-ionic fluids which is exact at low gas densities and so a suitable starting point is the OZ integral-equation which in terms of the chain function, $\gamma(r)$, is given by (Rushbrooke, 1968; Hansen and MacDonald, 1976; Lee, 1988; Rowlinson and Swinton, 1982; Reed and Gubbins, 1973).

$$\gamma(r_{12}) = \rho\int[\gamma(r_{13}) + c(r_{13})]c(r_{23})d\mathbf{r}_3;$$

Where, $\gamma(r_{12})$ $\{= h(r_{12}) - C(r_{12})\}$ is the chain function, ρ is the particle number density and $h(r_{12})$ is the total correlation function. Equation (2) is exact but intractable; therefore, to calculate $\gamma(r_{12})$ and $C(r_{12})$, the OZ equation must be supplemented by a closure which relates $\gamma(r_{12})$ and $C(r_{12})$. An exact but, again, intractable relationship between the two functions which is well suited for a discussion of the hypernetted chain (HNC) theory is

$$\ln y(r) = \gamma(r) + E(r);$$

Where, in the above we have employed the short-hand, $\gamma(r_{12}) = \gamma(r)$, etc. Equation (3) is not the most convenient route to the Percus-Yerick (PY) theory; for the latter one should write instead

$$c(r) = [1+\gamma(r)]f(r) + e(r)d(r); \qquad (4)$$

Scientia Africana, Vol. 14 (No.1), June 2015. Pp 165-177
© College of Natural and Applied Sciences, University of Port Harcourt, Printed in Nigeria *ISSN 1118 – 1931*

Where, in Eq. (4), $e(r)\{ = \exp(-\beta\phi(r))\}$ is the Boltzmann factor, $\beta\{= 1/kT\}$ is the reciprocal temperature, $f(r)\ \{ = e(r) - 1)$ is the Mayer function.

While in the first-order HNC theory, $E(r)$ in equation (3) is set identically equal to zero; in first-order PY theory it is $d(r)$ in equation (4) that is discarded. Our basic approach is to replace $E(r)$ in equation (3) with its first two accessible terms in the power series expansion of the function in density to obtain an extended HNC (or EHNC) approximation. Similarly, $d(r)$ is replaced with the first two accessible terms in its infinite series in density for an extended PY (or EPY) theory. Consequently, one obtains the following closures

EHNC: $$\ln y(r) = \gamma(r) + E^{(3)}(r) \quad (5)$$

EPY: $$c(r) = [1 + \gamma(r)] + e(r)d^{(3)}(r) \quad (6)$$

Where, for a LJ fluid

$$E^{(3)}(r) = \rho^2 E_2(r) + \rho^3 E_3(r) \quad (7)$$

$$d^{(3)}(r) = \rho^2 d_2(r) + \rho^3 d_3(r) \quad (8)$$

The graphs in $E^{(3)}(r)$ are a subset of those in $d^{(3)}(r)$ and these are displayed in Fgs 1 and 2, respectively.

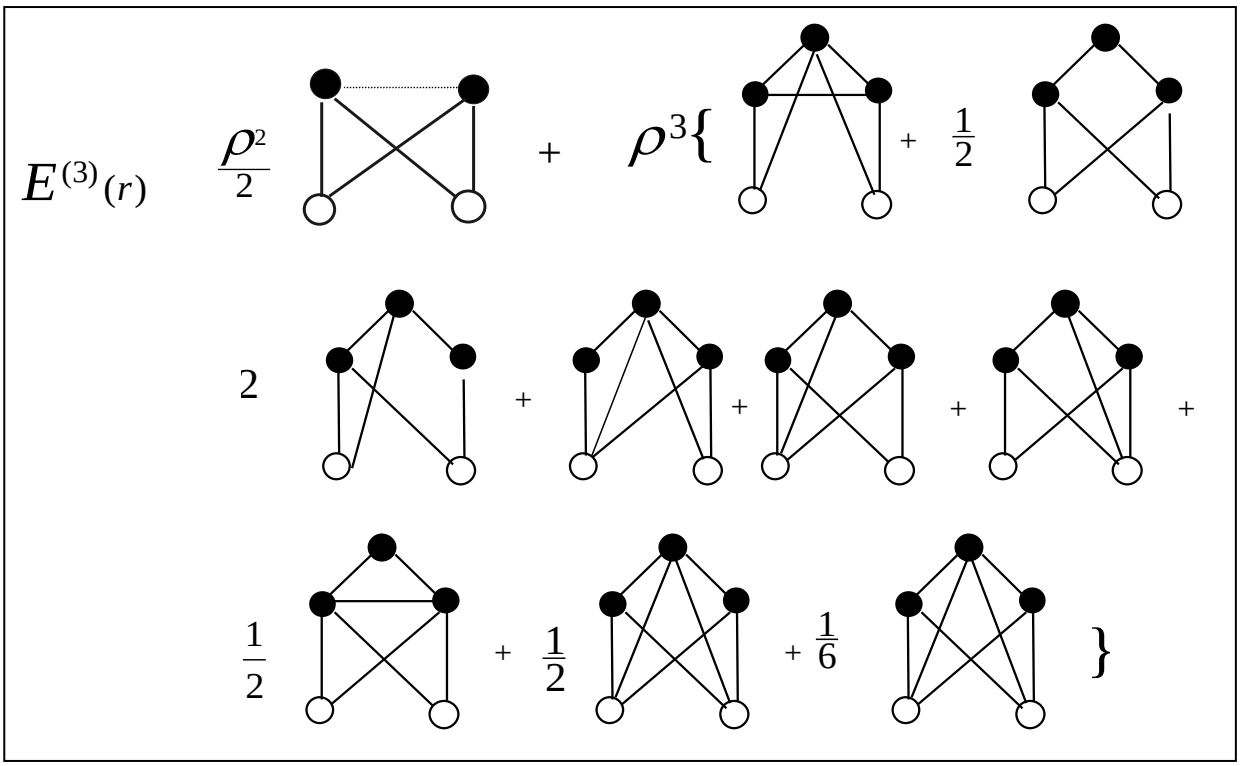

Fig1: Cluster diagrams that contribute to $E^{(3)}(r)$.

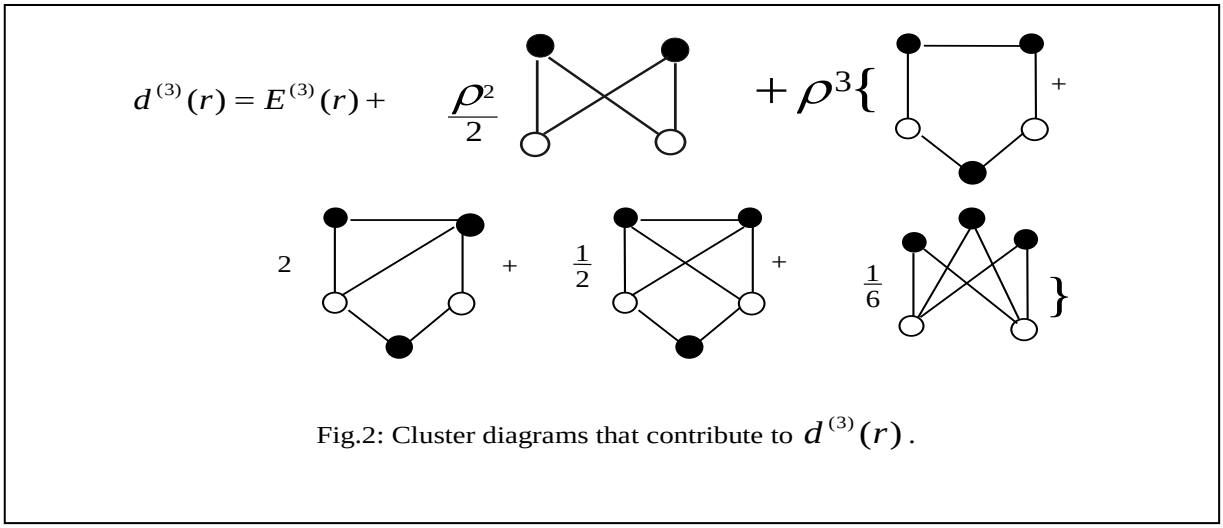

Fig.2: Cluster diagrams that contribute to $d^{(3)}(r)$.

Composite Graphs

Following Attard and Patey (1990), the tedium in calculating the graphs in $d^{(3)}(r)$ can be reduced considerably by forming composite graphs. Using this procedure, the graphs that one needs to evaluate to determine $d^{(3)}(r)$ are given in Fig. 3 (Monago, 1997).

Hence,

$$d^{(3)}(r) = \tfrac{1}{2}D_5^{(2)} + D_5^{(3)} + 2D_{6a}^{(3)} + \tfrac{1}{6}D_{6b}^{(3)} + \tfrac{1}{2}D_{7a}^{(3)} + 2D_{7b}^{(3)} + D_{7c}^{(3)} + \tfrac{1}{2}D_{9a}^{(3)} - \tfrac{1}{3}D_{9b}^{(3)} \quad (9)$$

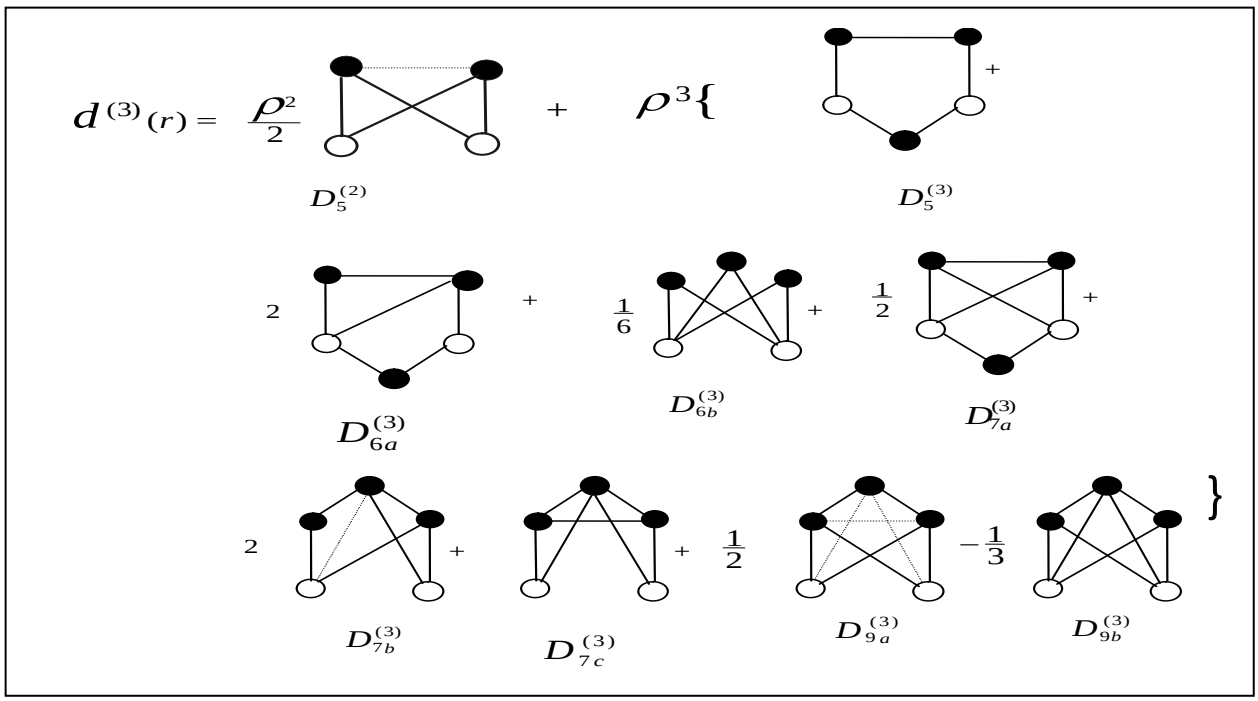

Fig. 3: The composite graphs in $d^{(3)}(r)$. In these graphs, each solid line represents an f-bond and a dotted line denotes an e-bond.

Scientia Africana, Vol. 14 (No.1), June 2015. Pp 165-177
© College of Natural and Applied Sciences, University of Port Harcourt, Printed in Nigeria *ISSN 1118 – 1931*

Integration of Graphs in $d^{(3)}(r)$

The method we use to expand and simplify the volume integrals represented by the graphs in Fig. 3 was that first employed by Barker and Monaghan (1996) and subsequently by several others (Henderson and Oden, 1996; Haymet and Rice, 1981). In that method, Mayer functions, which depend on the angles of integration in spherical polar co-ordinates, are expanded in Legendre polynomials. In what follows, we derive the computational expression for the complete rooted five-molecule graph and quote the results for the other graphs in table 1. Further details concerning the integration of the other graphs are given by Monago (1997).

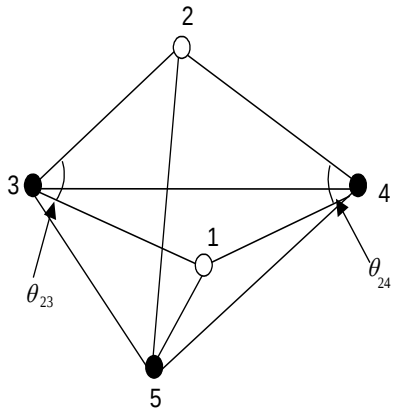

Fig. 4: Coordinate system for the rooted complete graph $D_{9b}^{(3)}$. φ_{34} is the angle between the planes 123 and 124; φ_{35} is that between 123 and 125.

In terms of the variables shown in Fig. 4:

$$\int d\mathbf{r}_3\, d\mathbf{r}_4\, d\mathbf{r}_5 = 2\pi\int_0^\infty r_{13}^2 dr_{13}\int_0^\infty r_{14}^2 dr_{14}\int_0^\infty r_{15}^2 dr_{15}\int_{-1}^1 dx_{23}\int_{-1}^1 dx_{24}\mathrm{x}$$
$$\int_{-1}^1 dx_{25}\int_0^{2\pi} d\varphi_{34}\int_0^{2\pi} d\varphi_{35}.$$

(10)

Where, $x_{23} = \cos\theta_{23}$; x_{24} and x_{25} are similarly defined. By definition,

$$D_{9b}^{(3)} = \int d\mathbf{r}_3\, d\mathbf{r}_4\, d\mathbf{r}_5\, f_{13} f_{14} f_{15} f_{23} f_{24} f_{25} f_{34} f_{35} f_{45}$$

. (11)

From equation (10) and (11) one obtains

$$D_{9b}^{(3)}(r) = 2\pi\rho^3\int_0^\infty r_{13}^2 f_{13} dr_{13}\int_0^\infty r_{14}^2 f_{14} dr_{14}\int_0^\infty r_{15}^2 f_{15} dr_{15}\int_{-1}^1 f_{23} dx_{23}\mathrm{x}$$
$$\int_{-1}^1 f_{24} dx_{24}\int_{-1}^1 f_{25} dx_{25}\int_0^{2\pi} d\varphi_{34}\int_0^{2\pi} d\varphi_{35} f_{34} f_{35} f_{45}.$$

(12)

It is convenient, in simplifying equation (12), to break the expression on the right-hand side into factors which will be considered sequentially. Let

$$F_3 = \int_0^{2\pi} d\varphi_{34}\int_0^{2\pi} d\varphi_{35} f_{34} f_{35} f_{45}. \qquad (13)$$

The Mayer functions in the above integral can be expanded in Legendre polynomials (Monago, 1997); we use f_{34} to fix ideas

$$f_{34}(r_{34},\theta_{34}) = \sum_{l=0}^{\infty} a_l(r_{13}, r_{14}) P_l(x_{34}), \qquad (14)$$

with

$$a_l(r_{13},r_{14})=\frac{2l+1}{2}\int_{-1}^{1} f_{34}P_l(x_{34})dx_{34}. \quad (15)$$

Hence,

$$F_3=\int_0^{2\pi}d\varphi_{34}\int_0^{2\pi}d\varphi_{35}\sum_{l,n,m=0}^{\infty}a_l(r_{13},r_{14})a_n(r_{13},r_{15})a_m(r_{14},r_{15})\mathrm{x}$$

$$\left[\sum_{s_1}^{l}(l,s_1)\delta_{s_1}P_l^{s_1}(x_{23})P_l^{s_1}(x_{24})\cos s_1\varphi_{34}\right]\mathrm{x}$$

$$\left[\sum_{s_2}^{n}(n,s_2)\delta_{s_2}P_n^{s_2}(x_{23})P_n^{s_2}(x_{25})\cos s_2\varphi_{35}\right]\mathrm{x}$$

$$\left[\sum_{s_3}^{m}(m,s_3)\delta_{s_3}P_m^{s_3}(x_{24})P_m^{s_3}(x_{25})\cos s_3\varphi_{45}\right]. \quad (16)$$

In equation (16), P_l^s is the associated Legendre polynomial and the following short-hand was used.

$$(\ell,s_1)=\frac{(\ell-s_1)!}{(\ell+s_1)!};$$

and

$$\delta_{s_1}\begin{cases}=1, & s_1=0\\ =2, & s_1>0\end{cases}$$

$(n,s_2),(m,s_3),\delta_{s_2}$ and δ_{s_3} are similarly defined. In equation (16), the integration of products of Legendre polynomials over 2π give zero unless $s_1=s_2=s_3=s$ in which case the result is π (Barker et al., 1996). Therefore,

$$F_3=\sum_{l,n,m=0}^{\infty}a_l(r_{13},r_{14})a_n(r_{13},r_{15})a_m(r_{14},r_{15})\sum_{s=0}^{\min(l,m,n)}(l,s)(m,s)(n,s)\mathrm{x}$$

$$\delta_s P_l^s(x_{23})P_n^s(x_{23})P_l^s(x_{24})P_m^s(x_{24})P_n^s(x_{25})P_m^s(x_{25}). \quad (17)$$

Where, min(l,m,n) denotes the smallest of the integers l,m, and n.

Next, let

$$F_2=\int_{-1}^{1}f_{23}dx_{23}\int_{-1}^{1}f_{24}dx_{24}\int_{-1}^{1}F_3dx_{25}. \quad (18)$$

Equation (18) may be simplified, after substituting for F_3, if one uses the orthogonality property of the associated Legendre functions

$$\int_{-1}^{1}P_l^s(x)P_m^s(x)dx=\frac{2(l,s)'}{2l+1}\delta_{lm}; \quad (19)$$

where,

$(l,s)'=(l,s)^{-1}$ and δ_{lm} is the Kronecker delta defined in the usual way. The result is

$$F_2=(2\pi)^2\sum_{l,m,n=0}^{\infty}a_l(r_{13},r_{14})a_n(r_{13},r_{15})a_m(r_{14},r_{15})\mathrm{x}$$

$$\sum_{s=0}^{\min(l,m,n)}(l,s)(m,s)(n,s)\delta_s\sum_{i=0}^{\infty}a_i(r_{12},r_{13})W_{iln}^s\mathrm{x}$$

$$\sum_{j=0}^{\infty}a_j(r_{12},r_{14})W_{ilm}^s\sum_{k=0}^{\infty}a_k(r_{12},r_{15})W_{knm}^s. \quad (20)$$

In equation (20)

$$W_{iln}^s=\int_{-1}^{1}P_i(x_{23})P_l^s(x_{23})P_n^s(x_{23})dx_{23} \quad (21)$$

W_{jlm}^s and W_{knm}^s are similarly defined if x_{24} and x_{25} are substituted for x_{23}, respectively. Use of equation (20) in (12) gives the final result; namely

$$D_{9b}^{(3)}(r)=(2\pi)^3\sum_{l,m,n,i,j,k=0}^{\infty}\int_0^{\infty}r_{13}^2f_{13}dr_{13}\int_0^{\infty}r_{14}^2f_{14}dr_{14}\int_0^{\infty}r_{15}^2f_{15}dr_{15}\mathrm{x}$$

$$a_l(r_{13},r_{14})a_n(r_{13},r_{15})a_m(r_{14},r_{15})\sum_{s=0}^{\min(l,m,n)}(l,s)(m,s)(n,s)\delta_s\mathrm{x}$$

Scientia Africana, Vol. 14 (No.1), June 2015. Pp 165-177
© College of Natural and Applied Sciences, University of Port Harcourt, Printed in Nigeria ISSN 1118 – 1931

$$a_i(r_{12}, r_{13}) a_j(r_{12}, r_{15}) a_k(r_{12}, r_{15}) W^s_{iln} W^s_{jlm} W^s_{knm}. \quad (22)$$

The corresponding expressions for the other five-molecule graphs in $d^{(3)}(r)$ are displayed in Table 1.

Numerical Computation of $d^{(3)}(r)$.

The cluster integrals in $d^{(3)}(r)$ were computed as part of a scheme that solved the OZ integral-equation; consequently, the integrals represented by the cluster diagrams were evaluated with various quadrature rules designed to achieve a compromise between speed and accuracy of the computation scheme.

For the four-molecule graphs, since we considered one-component systems, it was possible to reduce the computational effort by a factor of ½ by imposing the restriction $r_{13} \le r_{14}$. The projection coefficients a_l were evaluated from equation (15) according to the following scheme: first, the range of integration was divided into 7 equal panels, then each panel integration was performed by an 11-point Gaussian quadrature. In all cases, including the computation of five-molecule graphs, values of a_l were set equal to zero when $l > 11$. The semi-infinite integrals over r_{13} (or r_{14}) was truncated at $r = 9\sigma$, the integration itself was performed by Simpson's rule with N=200. The resulting numerical tabulation of $D_5^{(2)}(r)$ was on a coarse grid of spacing $\delta r = 9\sigma/200$ which was not adequate for use in calculating derived thermodynamic properties. To obtain adequate tabulation, a four-point Lagrange interpolation was performed on the coarse grid to obtain a fine one with the desired spacing (usually 0.015σ).

Table 1: Computational expressions for some five-molecule cluster integrals

Integral	Computational expression
$D_5^{(3)}(r)$	$2\pi h_1(r)\int_0^\infty h_1(r_{14})\Lambda\Lambda(r_{24})dr_{14}$
$D_{6a}^{(3)}(r)$	$2\pi h_1(r)\int_0^\infty h_1(r_{14})\Lambda\ (r_{24})f_{14}dr_{14}$
$D_{6b}^{(3)}(r)$	$[h_1(r)]^3$
$D_{7a}^{(3)}(r)$	$h_1(r).h_2(r)$
$D_{7b}^{(3)}(r)$	$16\pi^2\sum_{l=0}^{\infty}(\frac{1}{2l+1})^2\int_0^\infty \xi_{13}r_{13}^2dr_{13}\int_0^\infty f_{14}r_{14}^2dr_{14}a_l(r_{12},r_{13})\mathrm{x}$ $a_l(r_{12},r_{14})a_l(r_{13},r_{14})$
$D_{7c}^{(3)}(r)$	$(2\pi)^3\sum_{l,m,i,j=0}^{\infty}\left(\frac{2}{2m+1}\right)\int_0^\infty r_{13}^2dr_{13}\int_0^\infty r_{14}^2f_{14}dr_{14}\int_0^\infty r_{15}^2f_{15}dr_{15}\mathrm{x}$ $a_l(r_{13},r_{14})a_m(r_{13},r_{15})a_m(r_{14},r_{15})\mathrm{x}$ $\sum_{s=0}^{\min(l,m)}\delta_s(l,s)(m,s)a_i(r_{12},r_{13})a_j(r_{12},r_{14})W_{ilm}^sW_{jlm}^s.$
$D_{9a}^{(3)}(r)$	$(2\pi)^3\sum_{l,m,n,i,j,k=0}^{\infty}\int_0^\infty r_{13}^2f_{13}dr_{13}\int_0^\infty r_{14}^2e_{14}dr_{14}\int_0^\infty r_{15}^2f_{15}dr_{15}\mathrm{x}$ $a_l(r_{13},r_{14})b_n(r_{13},r_{15})a_m(r_{14},r_{15})\sum_{s=0}^{\min(l,m,n)}\delta_s(n,s)(m,s)(l,s)\mathrm{x}$ $a_i(r_{12},r_{13})b_j(r_{12},r_{14})a_k(r_{12},r_{15})W_{iln}^sW_{jlm}^sW_{knm}^s$
$\Lambda(r_{24})$	$\int_{1r_{12}-r_{14}l}^{r_{12}+r_{14}}r_{24}f_{24}dr_{24}$
$rh_1(r_{12})$	$2\pi\int_0^\infty \Lambda(r_{24})f_{13}r_{13}dr_{13}$
$r_{13}^2\xi(r_{13})$	$2\pi e_{13}r_{13}\int_0^\infty \Lambda(r_{35})f_{15}r_{15}dr_{15}$
$b_l(r_{13},r_{14})$	$\frac{2l+1}{2}\int_{-1}^{1}\beta\phi_{34}e_{34}P_l(x_{34})dx_{34}$

Scientia Africana, Vol. 14 (No.1), June 2015. Pp 165-177
© College of Natural and Applied Sciences, University of Port Harcourt, Printed in Nigeria *ISSN 1118 – 1931*

Radial integrations for all the five-molecule graphs were truncated at $r_{max} = 3.84\sigma$ and performed using Simpson's rule with 60 equal quadrature points. The graphs $D_5^{(3)}$, $D_{6a}^{(3)}$ and $D_{6b}^{(3)}$ were computed as written. For the rest of the five-molecule graphs, the projection coefficients a_l were tabulated as described above for the four-molecule graphs. The graphs $D_{7a}^{(3)}$ and $D_{7b}^{(3)}$ were computed as written except that in the case of $D_{7a}^{(3)}$ the computational effort was reduced by ½ as described for $D_5^{(2)}(r)$ above.

To evaluate the graph $D_{7c}^{(3)}(r)$, observe that {*i, j, l, m*} may assume integer values only and that W_{ilm}^{s} is zero unless $i \le l+m$ and the sum, {*i*+*l*+*m*}, is even. Similarly, W_{jlm}^{s} is zero unless $j \le l+m$ and the sum, (*j*+*l*+*m*), is even (Arfken and Weber, 1997). A sum in which either of the two restrictions above is violated is zero and need not be considered at all. If one examines all possible integer values in the set {*i,j,l,m*} having integer values between 0 and 11, a table of allowed sets {*i,j,l,m*} which make non-zero contributions to $D_{7c}^{(3)}(r)$ is easily prepared (Monago, 1997); a great deal of computational effort is saved by so doing.

It is even more imperative that one identifies the integer sets {*l,m,n,i,j,k*} that contribute finite sums to the cluster integrals $D_{9a}^{(3)}(r)$ and $D_{9b}^{(3)}(r)$. The following conditions are fulfilled in a valid set:
(a) $i \le l+n$ and the sum (*i*+*l*+*n*) is even;
(b) $i \le l+m$ and the sum (*i*+*l*+*m*) is even and
(c) $k \le n+m$ and the sum (*k*+*n*+m) is even.

More details, including a table of allowed values, may be found by Monago (1997).

Validation of the Computation Scheme

Analytical expressions for the magnitudes of the five-molecule graphs $D_{7c}^{(3)}(r)$ and $D_{9b}^{(3)}(r)$ for the Gaussian potential model are available from the work of Uhlenbeck and Ford (1962); those for the composite graphs $D_{7b}^{(3)}(r)$ and $D_{9a}^{(3)}(r)$ may be deduced from others listed in that publication. These are summarized in Table 2 below for convenience. The Gaussian potential is usually defined by its Mayer function

$$f(r) = -\exp\left(-\alpha r^2\right); \qquad (23)$$

where, $\alpha^3 = \frac{27}{8}\left(\pi/6\right)$.

Fig. 4 compares the magnitudes of four cluster integrals obtained from the present work against values from the analytical expressions for the Gaussian potential model given in table 2

Table 2: Analytical values of some five-molecule graphs for the gaussian potential [16,18]. $\Delta D_{3i} = D_i^{(3)}(\text{analytical}) - D_i^{(3)}(\text{numerical});\ \ i = 7b,\ 7c,\ 9a,\ 9b$

Graph	Expressions for the Gaussian potential.
$D_{7b}^{(3)}(r)$	$\left(\frac{4\pi}{3}\right)^3\left[\frac{\exp(-11/3)}{13^{3/2}} - \frac{\exp(-21/19)}{19^{3/2}}\right]\exp\left(-\alpha r^2\right)$
$D_{7c}^{(3)}(r)$	$-\left(\frac{2\pi^2}{27}\right)^{3/2}\exp\left(-7\alpha r^2/8\right)$
$D_{9a}^{(3)}(r)$	$\left(\frac{4\pi}{3}\right)^3\left\{\left(\frac{1}{12}\right)^{3/2} - \left(\frac{1}{20}\right)^{3/2} + \left[\left(\frac{1}{35}\right)^{3/2} - \left(\frac{1}{21}\right)^{3/2}\right]\text{x}\right.$ $\left. 2\exp\left(-\alpha r^2/7\right) + \left(\frac{1}{30}\right)^{3/2}\exp\left(-\alpha r^2/2\right)\right\}\exp\left(-\alpha r^2\right).$
$D_{9b}^{(3)}(r)$	$-\left(\frac{8\pi^2}{225}\right)^{3/2}\exp\left(-3\alpha r^2/2\right)$

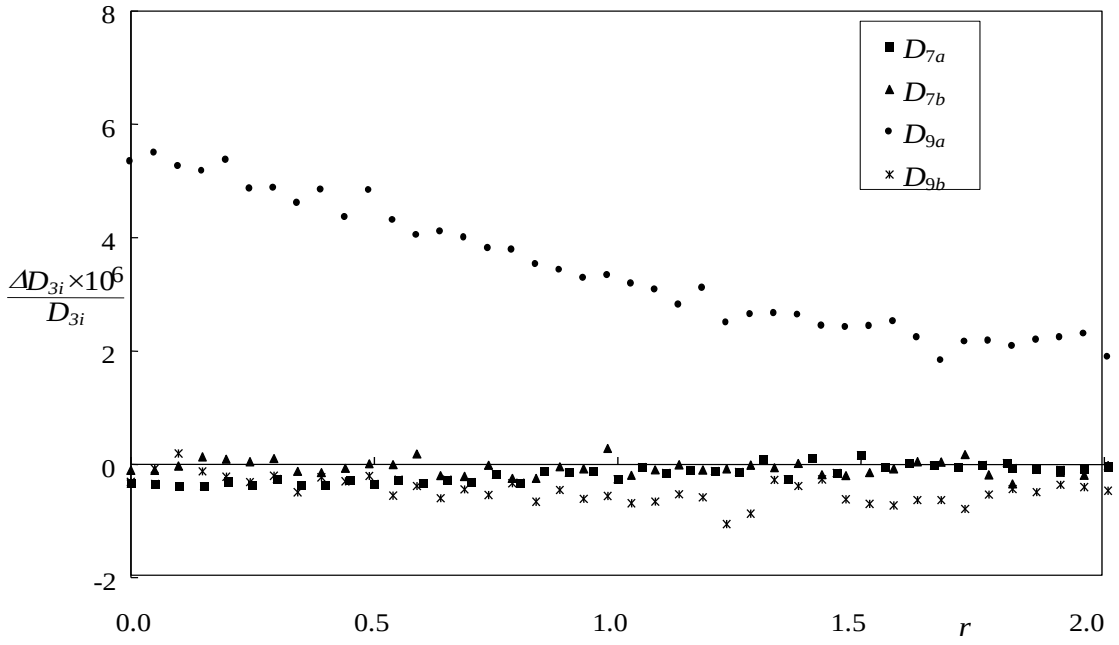

Fig5: Deviation plot for some five-molecule graphs when the analytical expressions in table2 are compared with derived computational expressions.

Scientia Africana, Vol. 14 (No.1), June 2015. Pp 165-177
© College of Natural and Applied Sciences, University of Port Harcourt, Printed in Nigeria *ISSN 1118 – 1931*

From each of the rooted graphs $D_5^{(3)}(r)$, $D_{6a}^{(3)}(r)$, $D_{6b}^{(3)}(r)$, $D_{7a}^{(3)}(r)$, $D_{7c}^{(3)}(r)$ and $D_{9b}^{(3)}(r)$ one can obtain the corresponding un-rooted graph in the 5*th* virial coefficient by inserting an f_{12} bond and integrating over $d\mathbf{r}_2$. The scheme is expressed in equation (24) – (29); the symbols on the left-hand-side are those used by Barker et al (1966).

$$E6\alpha = \int f_{12}\left[D_5^{(3)}(r)\right]d\mathbf{r} \quad (24)$$

$$E7\alpha = \int f_{12}\left[D_{6a}^{(3)}(r)\right]d\mathbf{r} \quad (25)$$

$$E7\alpha = \int f_{12}\left[D_{6b}^{(3)}(r)\right]d\mathbf{r} \quad (26)$$

$$E8\beta = \int f_{12}\left[D_{7b}^{(3)}(r)\right]d\mathbf{r} \quad (27)$$

$$E8\alpha = \int f_{12}\left[D_{7c}^{(3)}(r)\right]d\mathbf{r} \quad (28)$$

$$E10 = \int f_{12}\left[D_{9b}^{(3)}(r)\right]d\mathbf{r} \quad (29)$$

In table 3, the results obtained from Eq. (24)–(29) with a LJ potential are compared with the results of Barker et al. (1966). It is seen that except for the $E10$ and $E8\beta$ graphs at the lowest temperature where relative errors of some 11 per cent and 2.5 per cent, respectively, exist the calculations performed here agree with those of Barker et al. to better than 1 per cent.

Table 3: Calculated values of graphs in the 5*th* virial coefficient for a LJ potential model.

Graph	T^* = 0.75		T^* = 1.25	
	This work	ref. 13	This work	ref. 13
$E6\alpha$	152.568	152.5822	2.4060	2.3999
$E7\alpha$	-115.002	-114.773	-2.4548	-2.45671
$E7\gamma$	-62.662	-62.530	-1.8943	-1.89320
$E6\alpha$	-6.027	-6.075	-0.1088	-0.10961
$E6\beta$	-54.632	-53.290	0.3002	0.29945
$E10$	1.280	1.153	0.02805	0.02877

Graph	T^* = 1.6		T^* = 3	
	This work	ref. 13	This work	ref. 13
E6α	1.8976	1.89461	1.2096	1.21058
$E7\alpha$	-1.2941	-1.29406	-0.9853	-0.98639
$E7\gamma$	-0.6963	-0.69611	-0.2360	-0.2363
$E6\alpha$	0.0393	0.03895	0.1399	0.13995
$E6\beta$	0.4257	0.42506	0.3877	0.38812
$E10$	0.0123	0.0126	0.0081	0.0811

It is by no means certain that the calculations of Barker et al. for the complete (or K-) graph $E10$ should be preferred to the one performed here since they used only Legendre polynomials series with $l \leq 8$, while here we used $l \leq 11$. As shown by Henderson and Oden (1966) in the case of four-molecule graphs, truncating before l=11 can lead to non-negligible errors at low reduced temperatures. On the other hand, it should be pointed out that in the work of Barker et al. (1966) the radial integration was carried out to $r_{max}=20\sigma$. Even so, the discrepancy between the two results decline rapidly, even for the K-graph, at high reduced temperatures.

There are three main sources of error in the numerical computation of $d^{(3)}(r)$: truncation error due to the finite range of integration, truncation of the Legendre series and the error due to the finite grid spacing in the numerical integration. The sensitivity of the calculations performed here have been investigated with regards to independent variations in these parameters (Monago, 1997).

For the five-molecule graphs, when δr^*, $r_{\max}$ and $l_{\max}$ (for the Legendre polynomials) were perturbed by about 20 per cent, it was found that changes due to δr^* produced the greatest effects in the values of the graphs in the 5*th* virial coefficient at the lowest temperature considered here (i.e. $T^* = 0.75$). Table 4 shows the results for some five-molecule, unrooted graphs when $\delta r^*=0.04$, $T^*=0.75$; all other parameters pertaining to their computation remaining as for table 3.

Table 4: Sensitivity of Eq. (24)–(29) to the parameter δr^* at $T^*=0.75$.

Graph	Value	
	$\delta r^* = 0.05$	$\delta r^* = 0.04$
$E6\alpha$	152.568	152.228
$E7\alpha$	-115.002	-114.747
$E7\gamma$	-62.662	-62.513
$E6\alpha$	-6.027	-6.018
$E6\beta$	-54.632	-54.507
$E10$	1.280	1.278

As a result of similar tests on the computation scheme, it was concluded that the five-molecule graphs were computed with accuracy of better than 1 per cent at the lowest temperature. We feel that this level of error will negligibly impact on structural and thermodynamic properties bearing in mind that the relative contributions to these properties arising from the five-molecule cluster integrals are likely to be small.

A computational method to determine the coefficients, up to the third order, in the expansion of the tail of the direct correlation function in powers of density is described. It is based on expansion of Mayer functions in Legendre polynomials and it was demonstrated that, for realistic potentials, the method leads to reliable and accurate results at all temperatures. At the lowest temperature considered in this article ($T^* = 0.75$), the computational imprecision was estimated at about 1 percent; however, at the expense of greater computational costs, the method is capable of higher accuracy.

REFERENCES

Arfken, G. E. and Weber. H. J.(1995), "Mathematical Methods for Physicists", 2nd ed. (Academic press, int. ed.), p. 751.

Attard, P. (1989), "Spherically Inhomogeneous Fluids I. Percus-Yervick Hard Spheres: Osmotic Coefficients and Triplet Correlation", *J. Chem. Phys*., **91**, 3072 – 3082.

Attard, P and Patey, G. N.(1990), "Hypernetted-Chain Closure with Bridge Diagrams. Asymmetric Hard

Scientia Africana, Vol. 14 (No.1), June 2015. Pp 165-177
© College of Natural and Applied Sciences, University of Port Harcourt, Printed in Nigeria ISSN 1118 – 1931

Sphere Mixtures", *J. Chem., Phys*., **92**, 4970 – 4982.

Barker, J. A., Leonard, P. J. and Pompe, A., "Fifth Virial Coefficients", *J. Chem Phys*., 1966, **44**, 4206 – 4211.

Duh, D., Henderson, D, Mier-Y-Teran, L. and Sakolowski S.(1997), "Application of some Second-order Integral Equation Theories to the Lennard-Jones Fluids", *Mol. Phys*., **90**, 563 – 570.

Duh, D and Henderson, D.(1996), "Integral Equation Theory for Lennard-Jones Fluids: The Bridge Function and it's Applications to Pure Fluids and Mixtures", *J. Chem. Phys*., 1996, **104**, 6742 – 6754.

Duh, D and Haymet, A. D. J.(1995), "Integral Equation Theory for Uncharged Liquids: The Lennard-Jones Fluid and the Bridge Function", *J. Chem. Phys*., 1995, **103**, 2625 – 2633

Hansen J. P. and MacDonald, I. R.(1976), "Theory of Simple Fluids", Academic Press (London), p. 21

Haymet, A. D. J. and Rice, S. A.(1981), "An Accurate Integral Equation for the Pair and Triplet Distribution Functions of a Simple Liquid", *J. Chem. Phys*., **74**, 3033 – 3041.

Henderson, D. Kim, S. and Oden, L.(1967), "Exact and Approximate Values of the Distribution Functions of a Simple Fluid", *Discuss. Faraday Soc*., **43**, 26 – 31.

Henderson, D. and Oden, L.(1966), "Virial Expansion for the Radial Distribution Function of a Fluid Using the 6:12 Potential", *Mol. Phys*., **10**, 405 – 425.

Kim, S. Henderson, D. and Oden, L.(1969), "Exact Values for the Pair Distribution Function and Direct Correlation Function of a 6:12 Fluid at Low Density", *Trans. Faraday Soc*., **65**, 2308 – 2319.

Lee, L. L. (1988), "Molecular thermodynamics of non-ideal fluids", Butterworths, (London), p 97

Monago, K. O. (1997), "Thermodynamic Properties of Fluids by Integral-equation methods", Ph.D. thesis, University of London

Reed, T. M. and Gubbins, K. E. (1973), "Applied Statistical Mechanics", Butterworth-Heinemann (London), p. 58

Rowlinson, J. S. and Swinton, F. L. (1982), "Liquid and Liquid Mixtures", Butterworths (London), p 234

Rushbrooke, J. S. (1968), in "Physics of Simple Liquids", H. N. V. Temperley and J. S. Rowlinson (eds.), North-Holland (Amsterdam), pp 26 – 58

Uhlenbeck, G. E. and Ford, G. W..(1962), in "Studies in Statistical Mechanics", Vol. 1, J. De Boer and G.E. Uhlenbeck (eds.), North Holland (Amsterdam), pp 123 – 211.

Varlet, L.(1980), "Integral Equations for Classical Fluids I. The Hard Sphere Case", *Mol. Phys*., 1980, **41**, 183 – 190.

Wertheim, M.(1967)., "Integral Equations in the Theory of Classical Fluids", *J. Math. Phys*., **8**, 927 – 938.